Combustion Science and Technology

ISSN: 0010-2202 (Print) 1563-521X (Online) Journal homepage: http://www.tandfonline.com/loi/gcst20

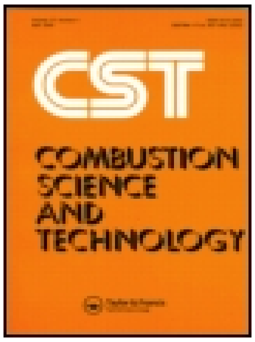

Oscillatory Burner-Attached Diffusion Flame in a Viscous Vortex

Milan Miklavcic & Indrek S. Wichman

To cite this article: Milan Miklavcic & Indrek S. Wichman (2018): Oscillatory Burner-Attached Diffusion Flame in a Viscous Vortex, Combustion Science and Technology, DOI: 10.1080/00102202.2018.1497018

To link to this article: https://doi.org/10.1080/00102202.2018.1497018

Published online: 30 Jul 2018.

COMBUSTION SCIENCE AND TECHNOLOGY
https://doi.org/10.1080/00102202.2018.1497018

Oscillatory Burner-Attached Diffusion Flame in a Viscous Vortex

Milan Miklavcic[a] and Indrek S. Wichman[b]

[a]Department of Mathematics, Michigan State University, East Lansing, Michigan, USA; [b]Department of Mechanical Engineering, Michigan State University, East Lansing, Michigan, USA

ABSTRACT

A method for mathematically solving the oscillatory infinite reaction rate diffusion flame is extended to the case where the oscillating convective coflow is either inside of, or adjacent to, a viscous vortex. The neglect of streamwise diffusion coupled with the restriction to infinite rate chemistry produces a Burke-Schumann boundary layer flame. The mathematical transformation, which does not require *a priori* restriction to small coflow oscillations, renders the transient oscillatory problem equivalent to a steady-state problem that can be solved mathematically and numerically evaluated to a high degree of accuracy. Flow fluctuations that are large fractions of the initial flow field are described exactly. Features of the flame response are examined without recourse to detailed time-dependent numerical simulations. There is no need to perform any small-perturbation analyses. The method is applied to examine the influences of the bulk inflow speed, the bulk inflow oscillation rate, and the interaction of the inflow and its oscillation rate with the viscous vortex.

ARTICLE HISTORY
Received 19 April 2018
Revised 2 July 2018
Accepted 2 July 2018

KEYWORDS
Diffusion Flames; Fire Whirls; Infinite Rate Chemistry; Oscillatory Flow; Exact Solution

Introduction and background

This article formulates a Burke-Schuman (B-S) model (Burke and Schuman, 1928) in order to examine burner-attached flames. The rotating burner flames are situated in a bulk flow that is both oscillatory *and* rotational, the oscillatory flow being along the flame axis, or length, and the rotation being in the direction of the main flame axis.

The B-S flame model has two distinct core features. (1) Negligible streamwise diffusion of species, thermal energy, and momentum. Thus, the B-S formulation is essentially a boundary-layer formulation (Schlichting and Gersten, 2000). (2) Infinitely fast flame chemistry. Thus, nonlinearities associated with reaction chemistry disappear from the problem.

The purpose of this study is to examine a particular case of the burner/whirl for which an exact mathematical solution can be developed and then used in order to examine the influence of the flow features on their structure and behavior. The intent of this work is to demonstrate that a simple model with a rigorous (exact) solution can provide important information about the basic structure of attached diffusion flames. The message is that a mathematical model, which can be solved analytically, can reproduce many important and possibly dominant flame characteristics and behaviors: adding more terms to the

CONTACT Indrek S. Wichman wichman@egr.msu.edu Department of Mechanical Engineering, Michigan State University, East Lansing, Michigan, USA

Color versions of one or more of the figures in the article can be found online at www.tandfonline.com/gcst.

equations enables the physics to be more accurately characterized but would also cloud the problem by making it impossible to solve using analytical techniques. Such a study would necessarily be numerical and dependent upon additional factors.

As background and justification, analytical models provide physical and mathematical information in the form of strict quantifiable relationships. This is one reason that the studies of Roper (1977a, 1977b) are still cited at an appreciable rate. Analytical models are important also for a more general reason: experiments and numerical simulations are described in the context of models whose predications allow a focused interpretation of the experimental measurements and numerical solutions in terms of these strict quantifiable relationships.

Historically, flame oscillations have been examined in many areas of combustion. One of these areas is microcombustion (Fernandez-Pello, 2002). The technical challenge is to insure continued combustion under strong heat-loss conditions. Another area, not unrelated to the first, is burner flame attachment. The classical problem is that of a fuel stream emitted into a coflow of surrounding oxidizer. In order to avoid complications caused by vortex trains populated with small, intense vortices (Roshko, 1976) researchers have examined jets in which the fuel and surrounding oxidizer have nearly similar coflow velocities. Issues of concern are flame heights, combustion rates, heat release, lame standoff distances, and conditions enabling blowoff. Fundamental studies on this topic have been conducted over many years, e.g. (Chung and Lee, 1991; Lee et al., 2003).

Regarding the control of combustion on burner-attached flames, the focus has been on understanding flame response to oscillating flow fields (Takahashi et al., 2007; Won et al., 2002). One control strategy is to increase flame surface, and therefore reactant consumption and heat release, by suitably modulating the oscillatory coflow (Magina et al., 2013). Exactly how much to oscillate the coflow, and in what fashion, remains a largely unanswered question.

Theoretical work on oscillating diffusion flames has examined flame response to both axial velocity and mixture fraction oscillations. The mixture fraction equation is customarily solved subject to the restriction to small flow perturbations (Preetham et al., 2010).

The configuration to be studied here considers an oscillating coflow velocity field that is also rotating. The rotational field, a viscous vortex, permits the development of an exact solution of the governing equations. A large inflow velocity makes diffusion in the x-direction irrelevant (which leads to the B-S model) and it also dwarfs the influences of buoyancy and entrainment. Consequently, the model studied here is meant to describe situations with a reasonably "large" inflow velocity. Situations with a low reactant inflow velocity will require including the effects of buoyancy, entrainment, and perhaps a low-speed transverse flow. These effects can currently only be characterized by experiments and massive numerical simulations.

Problem formulation

Consider the physical configuration shown in Figure 1. Fuel flows toward the positive x-direction through one or more channels that are each adjacent to one or more oxidizer channels. This configuration is called a slot burner (Azzoni et al., 1999; Gaydon and Wolfhard, 1979). For simplicity of analysis, the velocities in each of the channels are

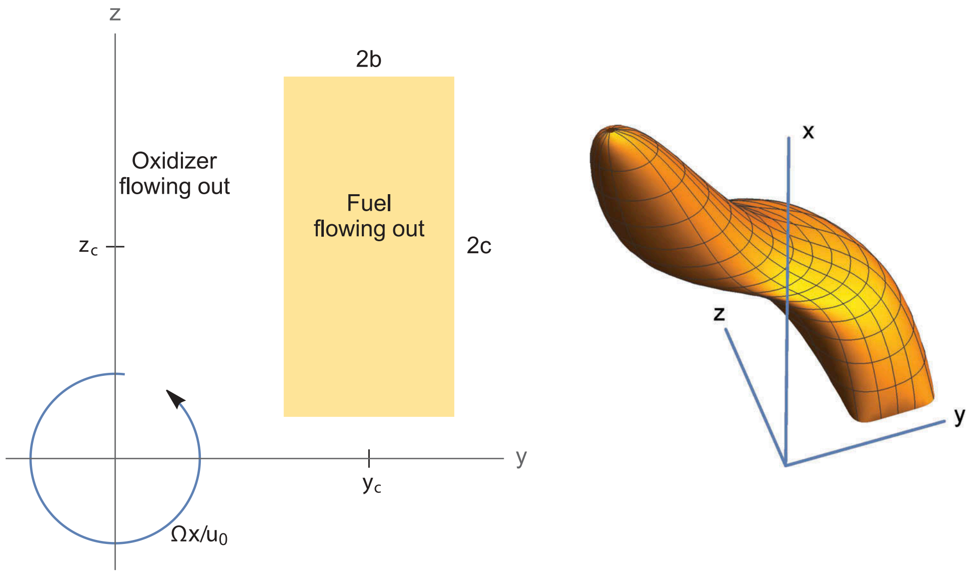

Figure 1. Fuel enters into the half-space $x > 0$ through an opening (or openings) surrounded by a coflowing stream of oxidizer. Rotation of the flow (Ω) is about the x-axis.

considered identical. For this reason, the formation of shear layers between adjacent channels is not considered. In addition to the streamwise flow the current work, in contrast to previous work (Miklavcic and Wichman, 2016), considers a rotational flow imposed on this jet-like burner.

As a physical background, the streamwise oscillating and transversely rotating flow field having velocity components $v_r = 0, v_\theta = r\Omega, v_x = u(t)$ satisfies the constant-density equation for conservation of mass, $(1/r)\partial(rv_r)/\partial r + (1/r)\partial v_\theta/\partial\theta + \partial v_x/\partial x = 0$. It also produces the following results for the Navier-Stokes momentum balance equations in cylindrical coordinates:

$$\frac{\partial p}{\partial r} = \rho r\Omega^2; \qquad \frac{\partial p}{\partial \theta} = 0; \qquad \frac{\partial p}{\partial x} = -\rho\frac{du_0(t)}{dt}. \tag{1}$$

These three equations integrate to give, for the pressure field $p(t, r, \theta, z) = \rho r^2\Omega^2/2 - \rho x du/dt + F(t)$, where $F(t)$ is a function of time. Thus, the velocity field $(0, r\Omega, u(t))$ satisfies the Navier-Stokes equations, as required.

Once the velocity field is known it remains for the B-S combustion analysis to solve the equation for the mixture fraction, Z, which is written as

$$\frac{\partial Z}{\partial t} + u\frac{\partial Z}{\partial x} + \Omega\frac{\partial Z}{\partial \theta} = D\left[\frac{1}{r}\frac{\partial}{\partial r}\left(r\frac{\partial Z}{\partial r}\right) + \frac{1}{r}\frac{\partial^2 Z}{\partial \theta^2}\right] = D\left[\frac{\partial^2 Z}{\partial y^2} + \frac{\partial^2 Z}{\partial z^2}\right]. \tag{2}$$

Here $v_\theta/r = \Omega$ and it is understood that the bulk fluid rotation rate Ω is constant. In Eq. (2) the Laplacian was equivalently written in cylindrical and Cartesian coordinates. Note that an alternative form of the derivative of Z with respect to θ, the polar angle in the $y - z$ plane measured counterclockwise from the y-axis, is given by

$$\frac{\partial Z}{\partial \theta} = y\frac{\partial Z}{\partial z} - z\frac{\partial Z}{\partial y}. \tag{3}$$

Solution

The mathematical transformation for the viscous swirling jet consists of two solution parts. The theoretical approach produces an exact relation between these parts, the first being a simpler steady, nonrotating "base" problem, the second being the unsteady, rotating "full" problem. The transformation yields the solution of the full problem in terms of the solution of the base problem. The method is outlined below for the problem with vorticity. Miklavic and Wichman (2016) provide the reader with a similar transformation for the simpler problem with no vorticity, i.e., $\Omega = 0$.

In addition to outlining the theoretical transformation, two additional mathematical details are provided. The first is the mathematical relationship between the base and full problems, including a calculation of the flame height and oscillation. The second is a description of the calculation of the transient, rotating flame surface.

Base problem (steady, no vorticity)

The base version of Eq. (2) is steady ($u(t) = u_0 = const$) and there is no vorticity ($\Omega = 0$). Thus,

$$u_0\frac{\partial Z_0}{\partial x} = D\left(\frac{\partial^2 Z_0}{\partial y^2} + \frac{\partial^2 Z_0}{\partial z^2}\right). \tag{4}$$

The base problem has many exact solutions. For example, for a single burner centered at the origin in the rectangular domain $|y| < b$ and $|z| < c$ the base solution is

$$\begin{aligned} 4Z_0(x,y,z) = {} & \left(\operatorname{erf}\frac{b-y}{\sqrt{4xD/u_0}} + \operatorname{erf}\frac{b+y}{\sqrt{4xD/u_0}}\right) \\ & \times \left(\operatorname{erf}\frac{c-z}{\sqrt{4xD/u_0}} + \operatorname{erf}\frac{c+z}{\sqrt{4xD/u_0}}\right). \end{aligned} \tag{5}$$

The base mixture fraction Z_0 satisfies

$$\lim_{x\to 0+} Z_0(x,y,z) = \begin{cases} 1 & \text{if } |y| < b \text{ and } |z| < c \\ 0 & \text{if } |y| > b \text{ or } |z| > c \end{cases} \tag{6}$$

at the exit plane, where the fuel stream is emitted into a coflowing infinite oxidizer stream having the same velocity. The solution given by Eq. (5) vanishes in the far field for any value of x, as required.

When Z_0 is obtained by Eq. (5), then $Z_0(x, y - y_c, z - z_c)$, which represents a burner with center at (y_c, z_c) in the exit plane $x = 0$, is also a solution of Eq. (4). Rotation of off-center flames produces flame whirls that will be discussed below. An example can be seen in Figure 1.

Note that any configuration of disjoint rectangular burners can be represented analytically by a superposition of appropriate modifications of Eq. (5). Therefor, the method outlined here provides a way to analyze quickly many different burner configurations.

The flame boundary of the infinite-rate chemistry diffusion flame is located at the position where the oxidant and fuel are in the stoichiometric ratio, or in other words, on the surface $Z = Z_{st}$. In practice, Z_{st} is typically small, of $O(10^{-1})$. The present calculations use $Z_{st} = 0.3$, as in Magina et al. (2013), but Z_{st} can be approximately $10\times$ smaller. Its smallness enables approximating the flame height H of a rectangular burner, Eq. (5), as follows:

$$Z_{st} = \operatorname{erf}\frac{b}{\sqrt{4HD/u_0}}\operatorname{erf}\frac{c}{\sqrt{4HD/u_0}} \approx \frac{bc}{\pi HD/u_0},$$

whereby

$$H \approx \frac{bcu_0}{\pi D Z_{st}}. \tag{7}$$

Full problem (unsteady, with vorticity)

The full mixture fraction Eq. (2) is solved subject to exit plane conditions, Eq. (6). The exact solution Z of Eq. (2) at time t and point (x, y, z) is found in terms of the exact base solution Z_0 of Eq. (4) at a point (ξ, η, ζ) as follows:

$$Z(t, x, y, z) = Z_0(\xi, \eta, \zeta), \tag{8}$$

where the new independent variables ξ, η, and ζ are given in terms of the full problem physical variables t, x, y, z by the relations

$$\xi = u_0 \cdot [t - S^{-1}(S(t) - x)], \tag{9}$$

$$\eta = y\cos(\Omega\xi/u_0) + z\sin(\Omega\xi/u_0), \tag{10}$$

$$\zeta = -y\sin(\Omega\xi/u_0) + z\cos(\Omega\xi/u_0). \tag{11}$$

Here the function $S(t)$ is defined as

$$S(t) = \int_0^t u(\kappa)d\kappa, \tag{12}$$

where κ is a dummy variable of integration. There is only one limitation to this transformation, as was discussed in Miklavcic and Wichman (2016): the flow must always exit the burner. Thus the fluctuating burner velocity can never produce a negative or backflow value for u.

To verify that Z given by Eqs. (8)–(11) satisfies Eq. (2) note first that

$$\xi_t = u_0 - u_0(S^{-1})'(S(t) - x)u(t), \eta_t = \zeta\Omega\xi_t/u_0$$

and

$$\zeta_t = -\eta\Omega\xi_t/u_0.$$

Hence

$$Z_t = (u_0 Z_{0\xi} + \Omega\zeta Z_{0\eta} - \Omega\eta Z_{0\zeta})\xi_t/u_0.$$

Then

$$\xi_x = u_0(S^{-1})'(S(t) - x), \eta_x = \zeta\Omega\xi_x/u_0, \zeta_x = -\eta\Omega\xi_x/u_0,$$

whereby

$$Z_x = (u_0 Z_{0\xi} + \Omega\zeta Z_{0\eta} - \Omega\eta Z_{0\zeta})\xi_x/u_0. \tag{13}$$

Use of the relation

$$\xi_t + u(t)\xi_x = u_0$$

in Eqs. (9)–(11) implies that

$$Z_t + u(t)Z_x = u_0 Z_{0\xi} + \Omega\zeta Z_{0\eta} - \Omega\eta Z_{0\zeta}.$$

Note also that

$$Z_y = Z_{0\eta}\cos(\Omega\xi/u_0) - Z_{0\zeta}\sin(\Omega\xi/u_0),$$

$$Z_z = Z_{0\eta}\sin(\Omega\xi/u_0) + Z_{0\zeta}\cos(\Omega\xi/u_0),$$

which imply that

$$zZ_y - yZ_z = \zeta Z_{0\eta} - \eta Z_{0\zeta}$$

and

$$Z_y^2 + Z_z^2 = Z_{0\eta}^2 + Z_{0\zeta}^2. \tag{14}$$

Knowing these relations, it is readily shown that $Z_{yy} + Z_{zz} = Z_{0\eta\eta} + Z_{0\zeta\zeta}$. The above results verify completely the entire transformation.

Relation between base and full problems

The goal of the above mathematical treatment is to describe flame shapes and behaviors. This goal is achieved by transforming the solution for the base flame via Eqs. (8)–(12) at the base flame point (ξ, η, ζ) in order to generate the unsteady, rotating flame boundary point (x, y, z) at time t. In order to see this clearly, it is necessary to invert Eqs. (9)–(11) to obtain, for the streamwise (x) flame coordinate the relation

$$x = S(t) - S(t - \xi/u_0), \tag{15}$$

and for the transverse (y) flame coordinate the relation

$$y = \eta \cos(\Omega\xi/u_0) - \zeta \sin(\Omega\xi/u_0) \tag{16}$$

and finally for the transverse (z) flame coordinate the relation

$$z = \eta \sin(\Omega\xi/u_0) + \zeta \cos(\Omega\xi/u_0). \tag{17}$$

Observe that Eq. (12) must yet be used in Eq. (15). The above transformation of individual points from the steady (and nonrotating) flow field to the unsteady (and rotating) flow field is valid for general exit velocity functions $u(t)$ subject only to the already-discussed physical constraint $u > 0$. Mathematically, violation of this constraint would render the transformation given by Eqs. (8)–(11) noninvertible. Thus, decaying velocity fields such as $u = u_0 e^{-\kappa t}$ are acceptable, as are turbulent velocity fields $u(t) = u_0 + u'(t)$, for example (Figure 6). As an illustrative and manageable special case, consider the regular, sinusoidally oscillating velocity field given by the simple function

$$u = u_0 + \varepsilon u_0 \cos \omega t. \tag{18}$$

In order to prevent backflow it must be true that $-1 < \varepsilon < 1$. However, ε does not need to be small as was required in previous studies based on perturbation theory, e.g., Magina et al. (2013), Preetham et al. (2010), and Tyagi and Jamadar (2007). Using this in Eq. (12) and then in Eq. (15) yields, for the streamwise position of any point in the transient rotating flow field,

$$x = \xi + \varepsilon\xi \frac{\sin \delta}{\delta} \cos(\omega t - \delta), \text{ where } \delta = \frac{\omega\xi}{2u_0}. \tag{19}$$

A point on the flame surface of any steady diffusion flame at a distance ξ above the plate will oscillate in the x-direction according to Eq. (19) when subjected to the bulk velocity flow Eq. (18) and any rotation. Note that the amplitude of the oscillations is zero when $\delta = n\pi$, i.e., when $\xi = 2n\pi u_0/\omega$. This defines nodal planes that are $2\pi u_0/\omega$ apart, see Figure 2. (Note: physical variables are all in the cgs system.) A rectangular burner with flame height given by Eq. (7) has the

$$\text{number of nodal planes } \approx \frac{bc\omega}{2\pi^2 Z_{st} D}. \tag{20}$$

The vorticity Ω rotates the flame boundary point (ξ, η, ζ) of any steady diffusion plane through the angle $\Omega\xi/u_0$ about the ξ-axis. For a rectangular burner having flame height given by Eq. (7) the number of

$$\text{rotations of the top of the flame } \approx \frac{bc\Omega}{2\pi^2 Z_{st} D}. \tag{21}$$

Figure 4 illustrates a flame on a narrow burner, having small Ω and strongly oscillating bulk velocity. When $\Omega = \omega$ a resonance appears between the bulk rotation and streamwise oscillation rates as illustrated in Figure 5.

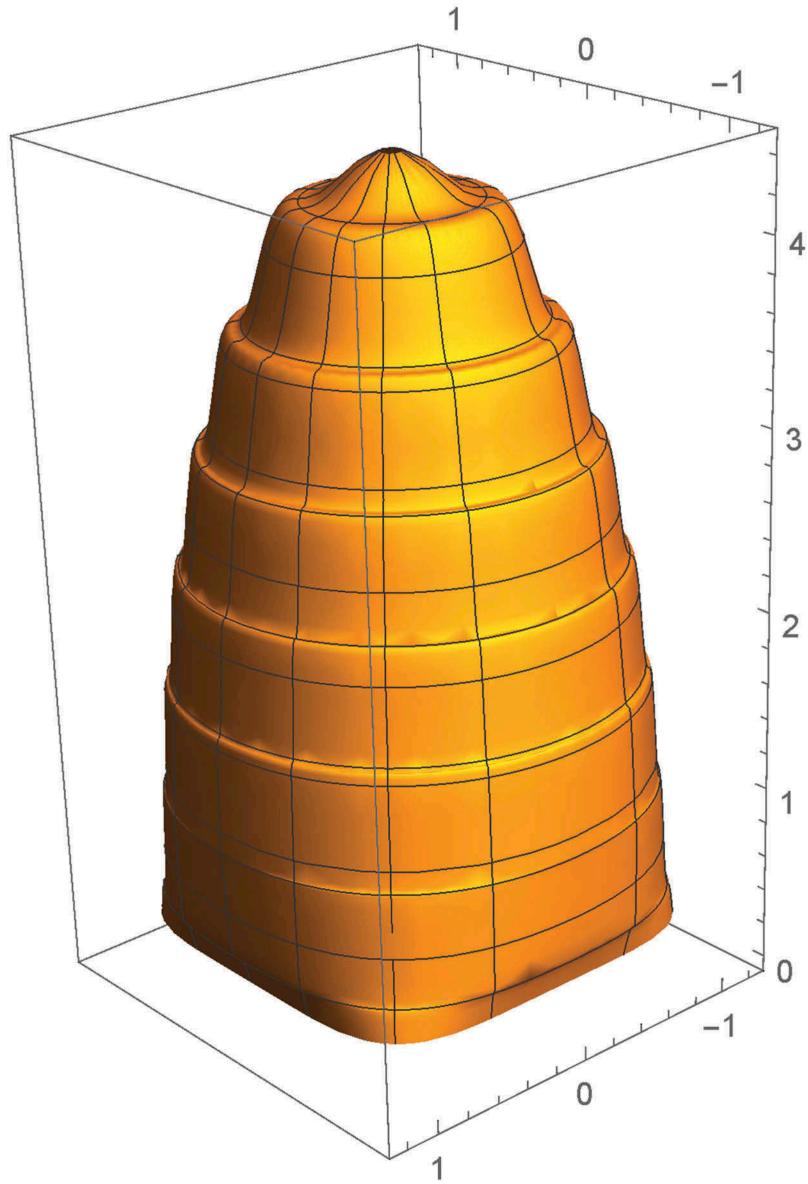

Figure 2. Seven (7) nodal planes with no rotation ($\Omega = 0$). $b = c = 1cm$ cm, $D = 1cm^2/s$cm^2/s, $u_0 = 5cm/s$ cm/s, $\omega = 50s^{-1}$ s^{-1}, $\varepsilon = 0.99$. Note the closeness of ε to unity, meaning *large* flow perturbations.

Flame surface area

This subsection shows the calculation of the flame surface area, which is proportional the reactant consumption rate. The boundary of the base flame surface $Z_0(\xi, \eta, \zeta) = Z_{st}$ is parametrized by using ξ and one other parameter, φ. Different parts of the surface may require different parametrizations. A viable choice is $\varphi = \theta$, the polar angle in the transverse plane at the height ξ. Choosing $\varphi = \eta$ is also possible. At the flame sheet

$$Z_0(\xi, \eta(\xi, \varphi), \zeta(\xi, \varphi)) = Z_{st}. \tag{22}$$

Equations (15)–(17) give the position vector on the boundary of the full flame surface as

$$\vec{r} = (S(t) - S(t - \xi/u_0), \eta\cos(\Omega\xi/u_0) - \zeta\sin(\Omega\xi/u_0), \eta\sin(\Omega\xi/u_0) + \zeta\cos(\Omega\xi/u_0)) \tag{23}$$

and hence $\vec{r} = \vec{r}(\xi, \varphi)$ is a parametrization of the full flame surface at time t. The surface area is

$$A(\Omega, t) = \int |\vec{r}_\xi \times \vec{r}_\varphi| \delta\xi\delta\varphi. \tag{24}$$

A lengthy calculation using Eq. (23) yields

$$|\vec{r}_\xi \times \vec{r}_\varphi|^2 = (\zeta_\xi\eta_\varphi - \eta_\xi\zeta_\varphi + (\eta\eta_\varphi + \zeta\zeta_\varphi)\Omega/u_0)^2 + (\eta_\varphi^2 + \zeta_\varphi^2)(u(t - \xi/u_0)/u_0)^2. \tag{25}$$

Using Eq. (22) enables writing

$$\eta_\varphi = -\lambda Z_{0\zeta}/Z_{0\xi}, \quad \zeta_\varphi = \lambda Z_{0\eta}/Z_{0\xi}, \tag{26}$$

where $\lambda = \zeta_\xi\eta_\varphi - \eta_\xi\zeta_\varphi$. Now using Eq. (26) in Eq. (25) yields

$$|\vec{r}_\xi \times \vec{r}_\varphi|^2 = \frac{\lambda^2}{u_0^2 Z_{0\xi}^2}[(u_0 Z_{0\xi} + \Omega\zeta Z_{0\eta} - \Omega\eta Z_{0\zeta})^2 + (Z_{0\eta}^2 + Z_{0\zeta}^2)u(t - \xi/u_0)^2]. \tag{27}$$

This describes the influence of Ω and $u(t)$ on the base flame surface area, Eq. (24), integrand. The calculations use $\eta = bR(\xi, \varphi)\cos\varphi$ and $\zeta = cR(\xi, \varphi)\sin\varphi$, which implies that $\lambda/Z_{0\xi} = bcR^2/[\eta Z_{0\eta} + \zeta Z_{0\zeta}]$ in Eqs. (26) and (27). These results are used to calculate exactly the flame surface area.

Scale analysis

In sections "Problem formulation" and "Solution," the analysis used the dimensional form because the transformations were readily interpreted in original variables. Additional information can be provided by forming dimensionless ratios for varying parameters and exploring proportionalities. Two approaches will be followed here. In the direct approach, the functional dependencies arise only from the governing equations. In the detailed approach, the nondimensionalization exploits theoretical results obtained directly from the mathematical formulas given in section "Solution."

Direct scaling

Define $\bar{t} = t/t_o, \bar{x} = x/a, \bar{y} = y/b, \bar{z} = z/c$ and $\bar{u} = u/u_o, \bar{\Omega} = \Omega/\Omega_o = 1, \bar{\omega} = \omega/\omega_o$. The ratio $c/b = A_R$ is the aspect ratio of the inflow slot. The characteristic time is chosen as the diffusion time, $t_o = c^2/D$. The characteristic length in the x-direction is $c = a^2u_o/D$, which gives, for Eq. (2),

$$\frac{\partial Z}{\partial \bar{t}} + \Delta \frac{\partial Z}{\partial \theta} + \bar{u}\frac{\partial Z}{\partial \bar{x}} = \frac{\partial^2 Z}{\partial \bar{y}^2} + \frac{1}{A_R^2}\frac{\partial^2 Z}{\partial \bar{z}^2}. \tag{28}$$

Parameter $\Delta = \Omega^2/D = t_{diff}/t_{rot} = (a^2/D)/(1/\Omega)$ and the limit $\Delta \to 0$ yields nonrotating flow. The limit $A_R \to \infty$ produces a slot burner, as does the limit $A_R \to 0$. These limits may be taken separately or jointly. The case $\Delta \to 0$ and $A_R \to \infty$ for the nonrotating slot jet was examined in Miklavcic and Wichman (2016). When c is interpreted as the flame height H the sole remaining length scale becomes $a = [RePrLe]^{-1/2}$, where $Re = u_0 H/\nu, Pr = \nu/\alpha$ and $Le = \alpha/D$.

Detailed scaling

The above pedestrian nondimensionalization is augmented with theoretical results from sections "Base problem (steady, no vorticity)," "Full problem (unsteady, with vorticity)," and "Relation between base and full problems" made possible by the base-to-full transformation given by Eq. (8). The relevant characteristic flame height is given from the solution at the end of section "Base problem (steady, no vorticity)" in Eq. (7). The flame lateral dimensions are defined as $b = l$ and $c = A_R l$, hence the flame height is $H = (A_R/\pi Z_{st})(l^2 u_o/D)$. This can be used to scale the factor a in $\bar{x}$. Note that $H/l \propto u_o l/D = Pe_l$, which is the Peclet number and represents the ratio of inertial $(u_o l)$ and molecular diffusion (D): hence, the dimensionless flame height is proportional to Pe_l/Z_{st}. The fire whirl study of Kunawa et al. (2011) produced a dimensionless flame height that reduced, in the small-Z_{st} limit, to $Pe/4Z_{st}$.

Temporal scales are associated with streamwise oscillation, ω, and bulk rotation, Ω. The flow oscillation given by the sinusoidally oscillating velocity field of Eq. (18) has period $T_\omega = 2\pi/\omega$. The furthest nodal plane, which gives the flame height, is found from Eq. (19) when $(2\pi/T_\omega)H/2u_o = \pi$, giving $T_\omega = A_R l^2/\pi Z_{st} D$, which yields $H = u_o T_\omega$. The lengths of the intermediate nodal planes are given by H/n, where n is given by Eq. (20). Since these are proportional to H it is clear that as T_ω increases the separation between the nodal planes increases by the same amount. The temporal scale associated with the bulk rotation rate of the fluid is given by the constant $\Omega = 2\pi/T_\Omega$. If this rotation rate carries the top of the flame through one complete rotation at $x = H$ then $\Omega H/u_o = 2\pi$, or $T_\Omega = T_\omega$. Of course, there is no a priori reason the bulk rotation rate must have this value.

The above results can be rephrased. Consider first that the mixture fraction value $Z_{st} \ll O(1)$ at the stoichiometric surface (flame). Then define l as the characteristic transverse (y, z) length so that $A_R \sim O(1)$, and write the period as $T = l^2/\pi Z_{st} D$. The height of the flame is $H = u_o T$. If the period of u is τ, then there are τ/T equally spaced nodal planes in the flame. Finally, if τ_Ω is the period of the bulk rotation, then the top of the flame rotates τ_Ω/T times.

Discussion and conclusions

Figure 1 shows an off-set flame with the center of rotation outside the flame base. This displacement distorts the flame shape accordingly. Another example of the displacement effect is shown in Figure 3 from a 3/4 perspective. This flame lies on an arc of constant rotation rate and it terminates at a height $H \sim 15cm$ cm from Eq. (7). Equation (21) gives the number of rotations as 1.5, slightly different than the actual 1.4. Figure 4 shows a small aspect ratio $A_R = 10^{-1}$ flame. The difficulty here is that in the development leading to Eq. (7) one of the error function arguments (the one containing b) is 10 times larger than the other, hence linearization of the former is not feasible: instead of five nodal planes Eq. (20) gives 16.9; instead of one half-rotation Eq. (21) gives 1.5. The "turbulent" flame having random fluctuations shown in Figure 6 yields, from Eq. (7), $H = 53.1cm$ cm, which is slightly larger than 40 cm shown in the figure. Again, $Z_{st} = 0.3$ is not "substantially smaller than unity" and therefore some discrepancy is expected. For this reason, Figure 5 produces $H = 106cm$ cm (larger than the 85 cm shown), and the number of nodal planes and flame-tip rotations 10.1 (larger than 7.7).

The influence of flow field oscillation on the flame surface area (and therefore on the reactant consumption rate and the flame heat release) were not discussed here, even though explicit formulas for the flame surface area were derived in section "Flame surface

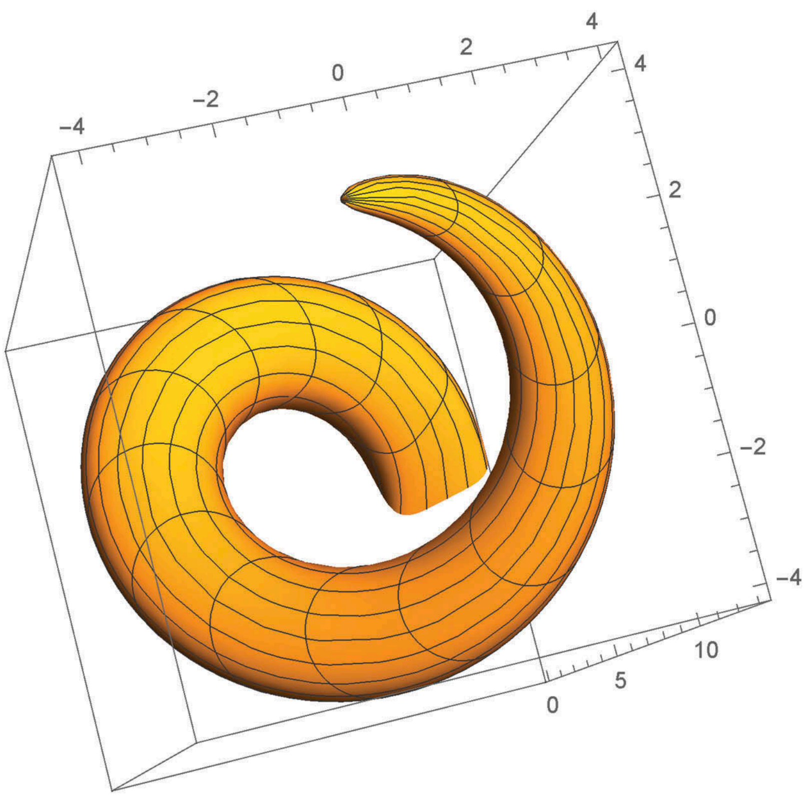

Figure 3. Flame showing 1.4 rotations, steady flow $u = u_0 = 15$. $b = c = 1$, rotation center at (3,0), $D = 1$, $\Omega = 9$. All units are cgs.

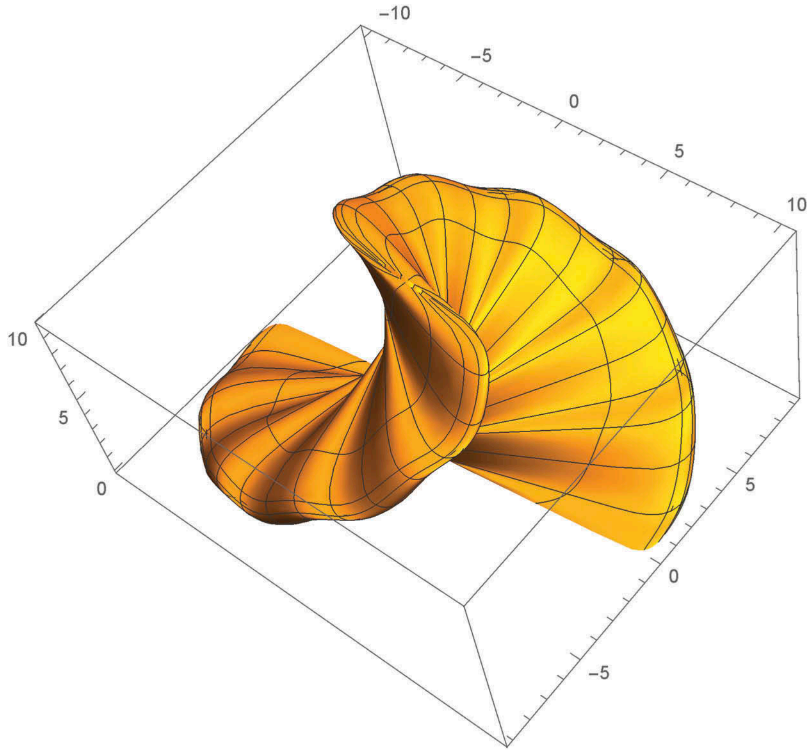

Figure 4. Small aspect ratio 0.1 with $b = 10$, $c = 1$. Rotation around its center. Also $u_0 = 3$, $D = 1$, $\Omega = 0.9$, $\varepsilon = 0.99$, $\omega = 10$. There are five nodal planes, one-half rotation. All units are cgs.

area," and were clearly used in order to construct Figures 1–6. As seen from Eqs. (24) and (27), the flame area is proportional to the product $bc = l^2 A_R$.

A detailed analysis of flame area change was made for the simple slot flame in Miklavcic and Wichman (2016), where it was shown that the oscillation frequency ω and its intensity ε produce, in the solution, a nonlinear coupling (through a square term in the solution, e.g., Eq. (27)) that enhances the effect of each to greatly magnify the flame area. On the subject of velocity field oscillation intensity, the reader will have noticed in Figures 2, 4, and 5 that the fluctuation ε was 99% of the bulk flow u_0, which is hardly a small perturbation.

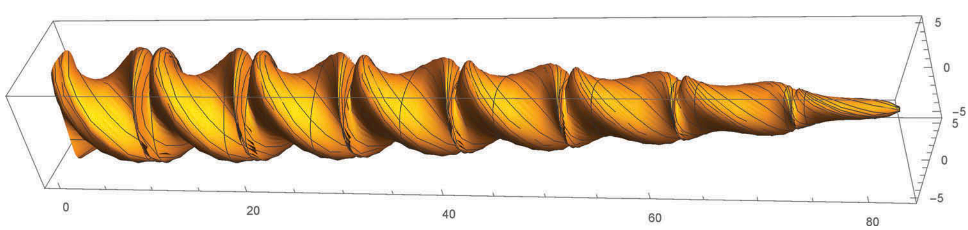

Figure 5. Aspect ratio 0.4 ($b = 5$, $c = 2$) with rotation about center. Also $u_0 = 10$, $D = 1$, $\Omega = \omega = 6$, and $\varepsilon = .99$ There are 7.7 nodal planes with 7.7 rotations over the flame height. Cgs units.

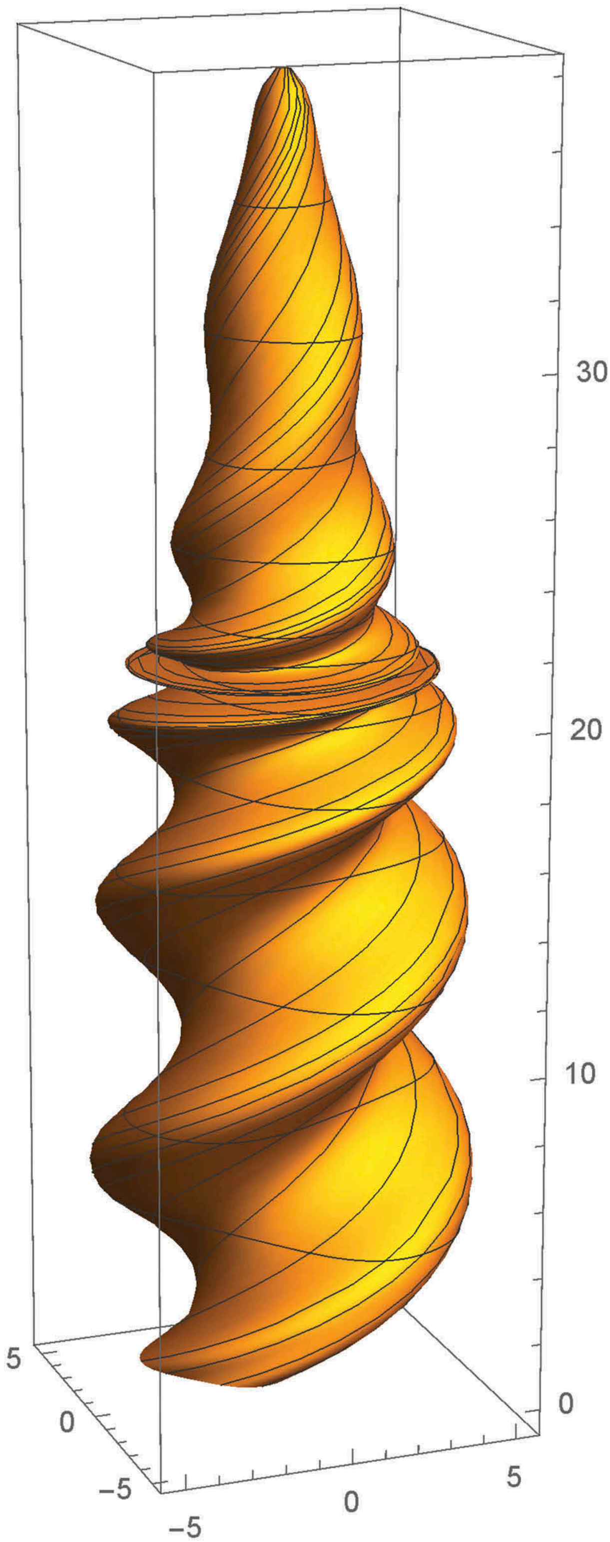

Figure 6. Rotating jet flame with randomly fluctuating bulk velocity u. Here $D = 1$, $u_0 = 5$, $\Omega = 3$, $b = 5$, and $c = 2$ in cgs units.

In the case of the burner flame, it is clear that the displaced flame in the viscous vortex will have a larger flame area since the height H is independent of the rotation rate. The analysis presented here makes possible the evaluation of large flow perturbations. Regarding the subject of fire whirls (Emmons, 1967), experimental research has shown strange and unexpected behaviors ranging from their movement over surfaces (see the references in Pinto et al. (2016)) (which implies the existence of a transverse flow velocity not in the current model) to issues of the merging of several flames, which the current model can address) to the issue of near-extinction whirls that produce small "horn" like shapes (Xiao et al., 2016). Buoyancy, which does not appear in the current model, plays a role in these flames and in their behavior. However, as discussed here, oscillatory motion of the surrounding flow also has a large influence unaccounted for in steady state models (Battaglia et al., 2000). Thus, although the current connection to fire whirls is tenuous, future research may determine various connections along the lines of Kunawa et al. (2011).

It is important to note, finally, that the construction of the mathematical solution has greatly simplified obtaining the numerical solution (and thus the figures shown here). In fact, almost all programming deals with finding the surface of the base, steady-state problem. The case of square burners requires, for example, only about 20 lines of code. For a group of four burners placed symmetrically would require approximately $O(100)$ lines of a code. To obtain the transient images (for the full problem) requires only about four more lines of code for each case. Thus, the method of solution presented here is computationally extremely efficient.

References

Azzoni, R., Ratt, S., Aggrawal, S.K., and Puri, I.K. 1999. The structure of triple flames stabilized on a slot burner. *Comb. Flame*, **119**, 23–40.

Battaglia, F., Rehm, R.G., and Baum, H.R. 2000. The fluid mechanics of fire whirls: an inviscid model. *Phys. Fluids*, **12**, 2859–2867.

Burke, S., and Schumann, T. 1928. Diffusion flames. *Ind. Eng. Chem*, **29**, 998–1004.

Chung, S., and Lee, B. 1991. On the characteristics of laminar lifted flames in a nonpremixed jet. *Comb. Flame*, **86**, 62–70.

Emmons, H., and Ying, S.J. 1967. The fire whirl. *Proc. Comb. Inst.*, **11**, 475–488.

Fernandez-Pello, A. 2002. Micropower generation using combustion: issues and approaches. *Proc. Comb. Inst*, **29**, 883–899.

Gaydon, A., and Wolfhard, H. 1979. *Flames: Their Structure, Radiation and Temperature*. 4th ed. Chapman and Hall, London.

Kuwana, K., Morishita, S., Dobashi, R., Chuah, K.H., and Saito, K. 2011. The burning rate's effect on the flame length of weak fire whirls. *Proc. Comb. Inst*, **33**, 2425–2432.

Lee, J., Won, S., Jin, S., and Chung, S. 2003. Lifted flames in laminar jets of propane in coflow air. *Comb. Flame*, **135**, 449–462.

Magina, N., Shin, D., Acharya, V., and Lieuwen, T. 2013. Response of non-premixed flames to bulk flow perturbations. *Proc. Comb. Inst.*, **34**, 963–971.

Miklavcic, M., and Wichman, I.S. 2016. Theoretical and numerical analysis of oscillating diffusion flames. *Comb. Flame*, **173**, 99–105.

Pinto, C., Viegas, D., Amleida, A., and Raposo, J. 2016. Fire whirls in forest fires: an experimental analysis. *Fire Safety J*, **87**, 37–48.

Preetham, K.T., Santosh, H., and Lieuwen, T. 2010. Linear response of laminar premixed flames to flow oscillations: unsteady stretch effects. *J. Prop. Power*, **26**, 524–532.

Roper, F. 1977a. The prediction of laminar jet diffusion flame sizes: part I. theoretical model. *Combust. Flame*, **29**, 219–226.

Roper, F. 1977b. The prediction of laminar jet diffusion flame sizes: part II. experimental verification. *Comb. Flame*, **29**, 227–234.

Roshko, A. 1976. Structure of turbulent shear flows: a new look. *AIAA J.*, **14**, 1349–1357.

Schlichting, H., and Gersten, K. 2000. *Boundary Layer Theory*. 8th ed. Springer, Berlin.

Takahashi, F., Linteris, G., and Katta, V. 2007. Vortex-coupled oscillations of edge diffusion flames in coflowing air with dilution. *Proc. Comb. Inst.*, **31**, 1575–1582.

Tyagi, M., Jamadar, N., and Chakravarthy, S. 2007. Oscillatory response of an idealized two-dimensional diffusion flame: analytical and numerical study. *Comb. Flame*, **149**, 271–285.

Won, S., Kim, J., Shin, M., Chung, S., Fujita, O., Mori, T., Choi, J.H., and Ito, K. 2002. Normal and microgravity experiment of oscillating lifted flames in coflow. *Proc. Comb. Inst*, **29**, 37–44.

Xiao, H., Gollner, M., and Oran, E. 2016. From fire whirls to blue whirls and combustion with reduced pollution. *Proc. Nat. Acad. Sci.*, **113**, 9457–9462.